


Inertial Force Transmission in Dense Granular Flows

Matthew Macaulay^{✉*} and Pierre Rognon^{✉†}

School of Civil Engineering, The University of Sydney, Sydney, NSW 2006, Australia

 (Received 24 November 2020; accepted 17 February 2021; published 18 March 2021)

Dense granular flows are well described by several continuum models; however, their internal dynamics remain elusive. This study explores the contact force distributions in simulated steady and homogenous shear flows. The results demonstrate the existence of high magnitude contact forces in faster flows with stiffer grains. A proposed physical mechanism explains this rate-dependent force transmission. This analysis establishes a relation between contact forces and grain velocities, providing an entry point to unify a range of continuum models derived from either contact forces or grain velocity.

DOI: [10.1103/PhysRevLett.126.118002](https://doi.org/10.1103/PhysRevLett.126.118002)

Granular flows transmit forces via a network of contacts between pairs of grains. Knowing the magnitude of these forces is key to predicting the dynamics of natural and industrial flows. First, contact forces are an elementary vector of momentum transport [1]. As such, they control the effective viscosity of the material. Second, large contact forces can lead to grain comminution, which in turns affects the flow microstructure and its rheological behavior [2]. However, while several continuum models can describe dense granular flows [3,4], the nature and the origin of their internal contact force distribution remain poorly understood.

Pioneering works focusing on quasistatic packings revealed that (i) the mean contact force is controlled by the confining stress P and the grain size d as Pd^2 and (ii) some contacts are compressed to much higher levels [5,6]. A piecewise force distribution was manifest, including an exponentially decaying probability of finding contact forces with a magnitude above the mean.

Contact forces in collisional flows are radically different as they arise from binary collisions between grains. In shear flows, Bagnold's scaling relates the typical impact velocity to the shear rate $\dot{\gamma}$ and the grain size d as $\dot{\gamma}d$. Considering a simple elastoinertial collision between grains of mass m and contact stiffness k provides an estimate for the maximum impact contact force of $\dot{\gamma}d\sqrt{km}$ [7]. This highlights a rate dependence of the contact forces.

In dense granular flows, binary collisions are seldom because grains typically experience multiple contacts. Their trajectories involve inertial reorganization events whose dynamics is independent on, and much faster than, the shear rate [3]. As a result, the grains' relative velocity deviates from Bagnold's scaling [8–10]. The resulting distribution in grain velocity has been shown to control the process of shear-induced diffusion [11,12]. However, how and whether it is related to contact forces are unknown.

In this Letter, we seek to establish a physically based model that captures the force distribution in dense granular

flows. In this aim, we have measured contact force distribution in simulated steady and homogenous shear flows and inferred a physical mechanism involving grain velocity fluctuations that is able to capture these observations.

Simulations.—We used a discrete element method to simulate granular flows in a plane shear configuration [Fig. 1(a)]. This configuration yields homogenous and steady flows that conveniently exude additional complexity arising in heterogenous or unsteady flows [13]. The shear cell is bidimensional. Both the normal stress P and the shear rate $\dot{\gamma}$ are prescribed using periodic boundary conditions [14] to avoid the flow heterogeneities that solid walls would induce [15]. The granular material comprises 10^4 grains of mean diameter d , mass m , and density ρ . A uniform polydispersity of $d \pm 20\%$ is introduced on the grain's diameter to prevent shear-induced crystallization. Grains interact via pairwise contacts including a normal elastodissipative force and a tangential friction. The Supplemental Material further details these granular interactions and the simulation procedure [16]. Contact parameters include a coefficient of restitution and a coefficient of friction, which are both set to 0.5. In contrast, different values of the contact normal stiffness k will be considered. The effect of these contact parameters on the granular rheology is discussed in [9].

The following analysis focuses on steady and homogeneous flows obtained with this configuration while prescribing two dimensionless numbers I and K :

$$I = \dot{\gamma}t_i; \quad t_i = d\sqrt{\frac{\rho}{P}}; \quad K = \frac{t_c^2}{t_i^2} = \frac{Pd}{k}. \quad (1)$$

The *inertial* number I compares the shear time $\dot{\gamma}^{-1}$ to the inertial time t_i . t_i measures a characteristic time for a grain of mass m initially at rest to move over a distance d under the action of a force Pd^2 [3,9]. The *softness* number K

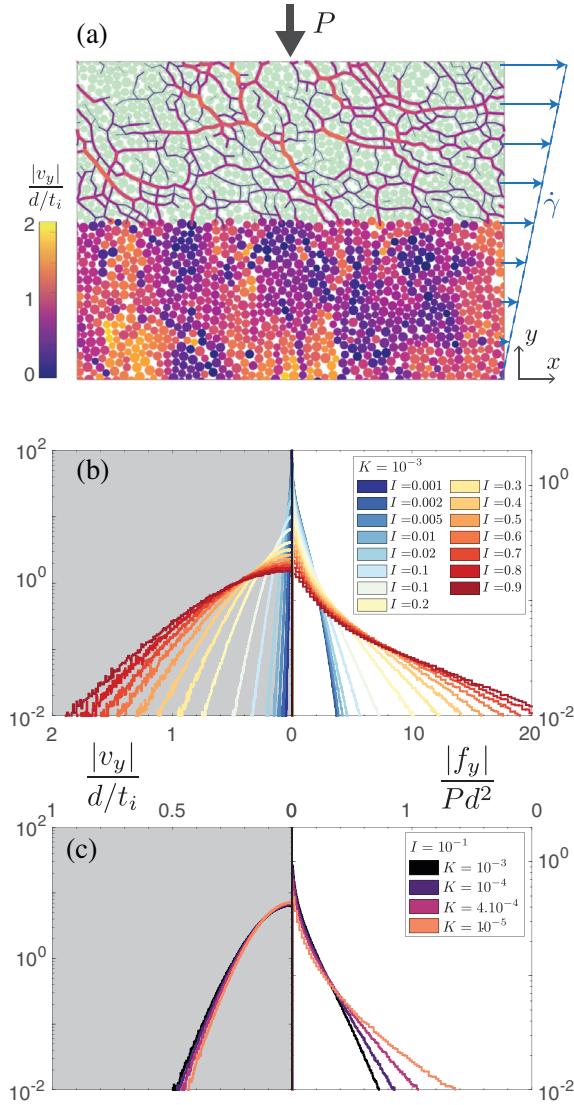


FIG. 1. Force and velocity distributions. (a) Plane shear under prescribed pressure P and shear rate $\dot{\gamma}$, showing a snapshot of the contact forces (top half; represented by segments of width proportional to the force magnitude) and of the grain velocities (bottom half) in a flow with $I = 0.01$ and $K = 10^{-3}$. Movies available in the Supplemental Material [16] show the evolution of contact forces and grain velocities within flows at different inertial number and softness. (b),(c) Probability density functions (PDFs) of grain velocity (left) and contact forces (right) for different inertial numbers [Fig. 1(b)] and different softness [Fig. 1(c)].

measures the elastic deformation of a grain experiencing a compressive contact force of magnitude Pd^2 ; equivalently, it compares the inertial time t_i to an elastoinertial collision time $t_c = d\sqrt{\rho d/k}$. In the following, results cover the ranges $10^{-3} \leq I \leq 0.9$ and $10^{-5} \leq K \leq 10^{-3}$, which correspond to the dense flow regime and the rigid limit, characterized by $t_c < t_i < \dot{\gamma}^{-1}$ [3,9].

Phenomenological scaling for force fluctuation.—First, we measured the component of the contact forces in the

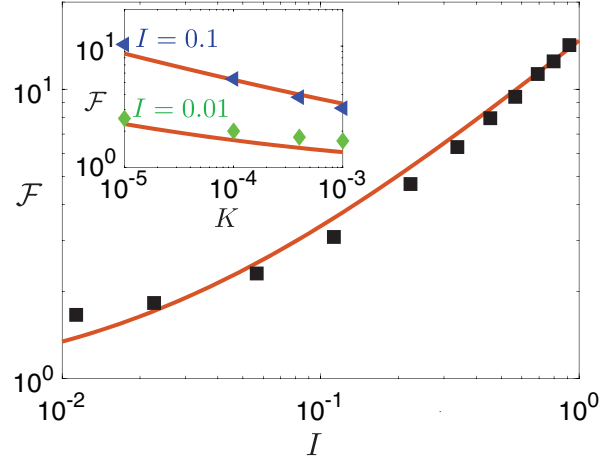


FIG. 2. Contact force fluctuations $\mathcal{F} = \delta F / Pd^2$ for different inertial numbers I ($K = 10^{-3}$, main) and different softness K (inset). Symbols, numerical results; and lines, proposed model [Eq. (4)].

direction transverse to the shear $|f_y|$ to determine their probability density function—the Supplemental Material shows that both components f_x and f_y have similar PDFs [16]. Taking advantage of the homogeneity and steadiness of the flows, these were measured by considering all grains in the cell and 300 sampled times spread evenly over 15 shear deformations. Figures 1(b) and 1(c) show that the force distributions are affected by both the inertial number I and the softness K . To characterize the width of these distributions, we measured their standard deviation δf , which we refer to as force fluctuation. Figure 2 shows the combined influence of I and K on the normalized force fluctuation $\mathcal{F} = \delta f / Pd^2$. δf converges to Pd^2 in the quasistatic limit $I \rightarrow 0$, which is consistent with the findings in [5,6]. In contrast, it becomes significantly larger at high inertial numbers and for stiffer grains: δf reaches values up to one order of magnitude larger than Pd^2 in the range of parameters that have been explored. However, these results do not immediately provide evidence for a relation between δf and the dimensionless numbers I and K .

To identify this relation, we use the microinertia theory introduced in [1] that relates contact force fluctuation to grain acceleration. The rationale for this theory is that multiple contact forces acting on a grain may be partially balanced. Their balanced part does not induce any acceleration and scales with Pd^2 . Their unbalanced part drives some grain acceleration according to Newton’s law of motion. This ultimately yields a linear relation between force and acceleration fluctuations $\delta f \approx Pd^2 + m\delta a$. Here, the acceleration fluctuation is defined as the standard deviation of the distribution in grain acceleration in the y direction. A dimensionless formulation of this relation is

$$\mathcal{F} \approx 1 + \mathcal{A}, \quad (2)$$

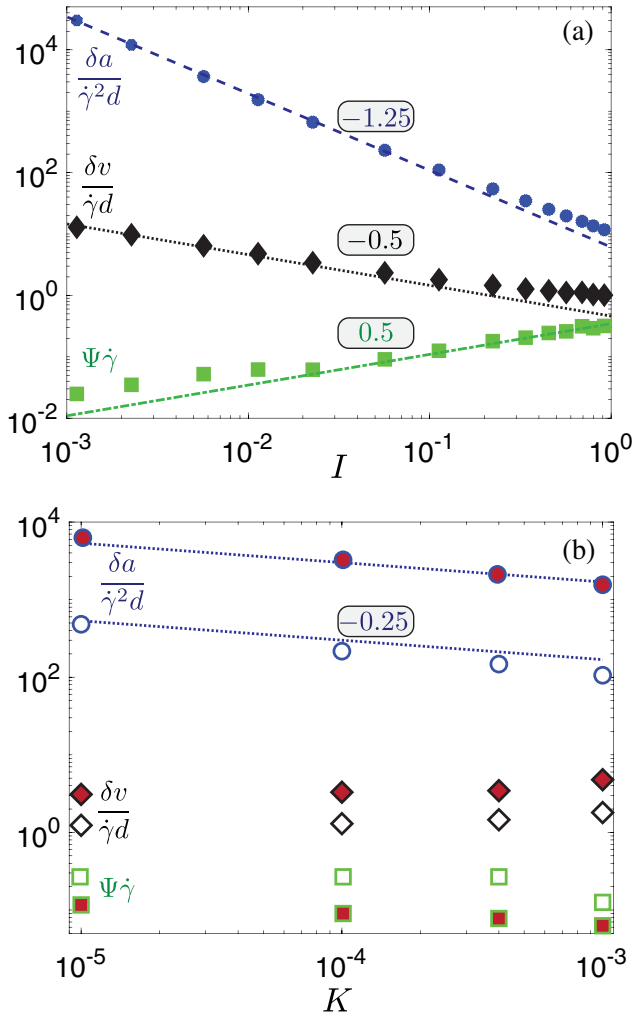


FIG. 3. Internal kinematic variables: Velocity fluctuation δv , acceleration fluctuation δa , and velocity memory time Ψ measured in flows with (a) different inertial numbers $K = 10^{-3}$ (results for $K = 10^{-4}$ are shown in the Supplemental Material [16], confirming the power laws), and (b) different softness K for $I = 10^{-2}$ (filled symbols) and $I = 10^{-1}$ (open symbols). Symbols, numerical results; and lines, proposed models in Eqs. (3), (5), and (6). Numbers summarize the power-law exponents.

where $\mathcal{A} = \delta a / (d/t_i^2)$ is the normalized acceleration fluctuation. The Supplemental Material [16] shows that this relation is valid for flows performed at different inertial numbers I and with different softness K . Thanks to this relation, establishing how the force fluctuation varies with I and K may be achieved by finding how the acceleration fluctuation varies with I and K .

Figure 3 shows that the acceleration fluctuation $\delta a/d\dot{\gamma}^2$ decreases with a higher inertial number and stiffer grains, seemingly with a power law:

$$\frac{\delta a}{d\dot{\gamma}^2} \propto K^{n_{aK}} I^{n_{aI}}. \quad (3)$$

Results are consistent with exponents $n_{aK} = -0.25$ and $n_{aI} = -1.25$. Introducing this scaling into the force-acceleration relation [Eq. (2)] leads to the following phenomenological scaling law for the force fluctuations:

$$\mathcal{F} \approx 1 + \alpha K^{-0.25} I^{0.75}. \quad (4)$$

Figure 2 shows that this relation reasonably captures the force fluctuation in the explored range of I and K with $\alpha = 2.5$ as a fitting parameter.

Physical process relating velocity and force fluctuations.—To identify a physical process at the origin of this phenomenological law, we now seek to relate the acceleration fluctuation to other kinematic quantities including grain velocities and their time persistence.

Figures 1(b) and 1(c) show that the grain vertical velocity distribution is affected by the inertial number. However, unlike contact forces, the velocity distribution is not dependent on the softness. Figure 3 reports the standard deviation of these distributions, which we refer to as velocity fluctuations δv . The results suggest the following power law:

$$\frac{\delta v}{\dot{\gamma}d} \approx 0.5 I^{n_v}. \quad (5)$$

As previously proposed [9,11,12], they are consistent with a power exponent $n_v = -0.5$. They further point out the negligible influence of the softness K .

Figure 3 also reports the velocity autocorrelation time Ψ , defined as

$$\Psi = \int_{t=0}^{\infty} \psi(t) dt,$$

where

$$\psi(t) = \langle v_y(t_0)v_y(t_0+t) \rangle / \langle v_y(t_0)^2 \rangle$$

is the velocity autocorrelation function, and the angle brackets denote the average operator on all grains and all reference times t_0 . We refer to Ψ as the velocity persistence time because it measures a characteristic period of time during which a grain velocity v_y is sustained. The persistence time is related to the coefficient of self-diffusion D by the Green-Kubo relation $D = \delta v^2 \Psi$ [12]. The results suggest the following power law:

$$\Psi \dot{\gamma} \approx 0.35 I^{n_\Psi}. \quad (6)$$

As previously reported [10–12], they are consistent with a power exponent $n_\Psi = 0.5$. They further highlight the near independence of the velocity memory time on the softness K .

From these two observations on the velocity fluctuation and their persistence, we infer a simplified scenario for a

typical grain motion in dense granular flows. Like a random walk, this scenario involves grains moving over steps of length $\delta v\Psi$ at a constant velocity δv before changing direction. Accordingly, the acceleration during the step is null. As for collisional flows, we postulate that the acceleration during the change of direction is of the order of $\delta v/t_c$: this reflects a change in grain velocity of $\pm\delta v$ in a period of time driven by the elastoinertial collision time t_c .

The characteristic mean square acceleration during such a cycle is (considering that $t_c \ll \Psi$)

$$\langle a^2 \rangle = \frac{(c\delta v/t_c)^2 t_c + 0}{\Psi} = \frac{\delta v^2}{t_c \Psi}.$$

This predicts the following relation between the velocity fluctuation and the acceleration fluctuation $\delta a \equiv \langle a^2 \rangle^{0.5}$:

$$\delta a \propto \frac{\delta v}{\sqrt{t_c \Psi}}. \quad (7)$$

Introducing this relation into the force-acceleration relation in Eq. (2) leads to the following relation between the force and velocity fluctuations:

$$\delta f - Pd^2 \propto m \frac{\delta v}{\sqrt{t_c \Psi}}. \quad (8)$$

Introducing in Eq. (8) the scalings for the velocity fluctuation and their lifetime in Eqs. (5) and (6) leads to the following scaling law for the force fluctuation expressed in terms of the inertial number and the softness K : $\mathcal{F} - 1 \propto K^{(-1/4)} I^{(3/4)}$, which is consistent with the phenomenological model [Eq. (4)]. The Supplemental Material [16] details this derivation and further assesses the validity of this scenario by comparing the measured δa and δf to the predictions of Eqs. (7) and (8), respectively.

Finally, Fig. 4 shows that the distribution of contact forces collapses onto a single exponential distribution when rescaled by the force fluctuation defined by Eq. (4). This distribution is similar to that found in quasistatic packings [5,6]. Here, we find how its width depends on the inertial number and grain softness in dense flows. Similarly, Fig. 4 shows that grain velocity distributions all collapse onto a single normal distribution when rescaled by the velocity fluctuation modeled by Eq. (5). This further confirms that, unlike contact forces, grain kinematic is independent on the softness K .

Conclusions.—This study highlights a significant rate dependence of contact forces in steady and homogeneous granular flows. It reveals the existence of forces much larger than the characteristic scale Pd^2 with an exponential distribution, and it introduces a model [Eq. (4)] to capture the width of this distribution as a function of the inertial number and grain softness. These results can be used to

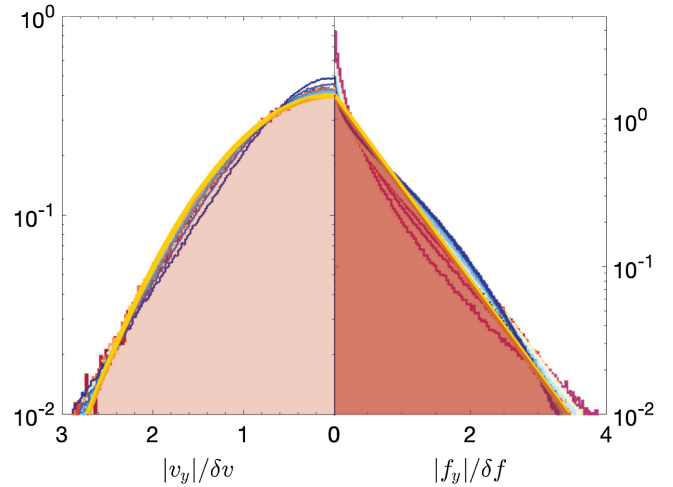


FIG. 4. Rescaling of force and velocity distribution. Lines are the PDFs presented in Figs. 1(b) and 1(c) rescaling grain velocity and contact forces by δv and δf defined in the models of Eqs. (5) and (4), respectively. Filled areas show a normal distribution $(2\pi)^{-(1/2)} e^{-(1/2)(|v_y|/\delta v)^2}$ (left) and an exponential distribution $e^{-\beta(|f_y|/\delta f)}$ (right) with $\beta = 1.4$ found as best fitting the data.

foresee flow conditions likely to lead to grain breakage or abrasive wear induced by extreme contact forces.

The random-walk mechanism introduced to explain this rate dependence of the force distribution highlights a relationship between contact forces and grain velocity fluctuation [Eq. (8)]. This relationship is an entry point to help reconcile two distinct existing approaches to understand the constitutive behavior of dense granular flows that are based on either contact forces [1,17,18] or grain velocity fluctuations [19–21]. In particular, establishing the validity—or deviation from—this relation in more complex geometry including volume-controlled, unsteady, or nonhomogeneous flows could help interpret the origin of rheological behaviors such as nonlocality. Finally, we anticipate that analogous physical processes could govern the force distribution in other soft materials such as suspensions, foams, and emulsions, which would involve each material’s specific mode of interaction working via an interstitial liquid.

This research was supported by the Australian Research Council (DP200101927).

*matthew.macaulay@sydney.edu.au

†pierre.rognon@sydney.edu.au

- [1] M. Macaulay and P. Rognon, Two mechanisms of momentum transfer in granular flows, *Phys. Rev. E* **101**, 050901(R) (2020).
- [2] B. Marks and I. Einav, A mixture of crushing and segregation: The complexity of grainsize in natural granular flows, *Geophys. Res. Lett.* **42**, 274 (2015).
- [3] G. MiDi, On dense granular flows, *Eur. Phys. J. E* **14**, 341 (2004).

- [4] K. Kamrin and G. Koval, Nonlocal Constitutive Relation for Steady Granular Flow, *Phys. Rev. Lett.* **108**, 178301 (2012).
- [5] F. Radjai, D. E. Wolf, M. Jean, and J.-J. Moreau, Bimodal Character of Stress Transmission in Granular Packings, *Phys. Rev. Lett.* **80**, 61 (1998).
- [6] T. S. Majmudar and R. P. Behringer, Contact force measurements and stress-induced anisotropy in granular materials, *Nature (London)* **435**, 1079 (2005).
- [7] M. Macaulay and P. Rognon, Viscosity of cohesive granular flows, *Soft Matter* **17**, 165 (2021).
- [8] F. Radjai and S. Roux, Turbulentlike Fluctuations in Quasistatic Flow of Granular Media, *Phys. Rev. Lett.* **89**, 064302 (2002).
- [9] F. da Cruz, S. Emam, M. Prochnow, J.-N. Roux, and F. Chevoir, Rheophysics of dense granular materials: Discrete simulation of plane shear flows, *Phys. Rev. E* **72**, 021309 (2005).
- [10] E. DeGiuli, J. McElwaine, and M. Wyart, Phase diagram for inertial granular flows, *Phys. Rev.* **94**, 012904 (2016).
- [11] P. Kharel and P. Rognon, Vortices Enhance Diffusion in Dense Granular Flows, *Phys. Rev. Lett.* **119**, 178001 (2017).
- [12] M. Macaulay and P. Rognon, Shear-induced diffusion in cohesive granular flows: Effect of enduring clusters, *J. Fluid Mech.* **858**, R2 (2019).
- [13] F. V. Reyes, A. Santos, and V. Garzó, Non-Newtonian Granular Hydrodynamics. What do the Inelastic Simple Shear Flow and the Elastic Fourier Flow Have in Common?, *Phys. Rev. Lett.* **104**, 028001 (2010).
- [14] A. Lees and S. Edwards, The computer study of transport processes under extreme conditions, *J. Phys. C* **5**, 1921 (1972).
- [15] P. G. Rognon, T. Miller, B. Metzger, and I. Einav, Long-range wall perturbations in dense granular flows, *J. Fluid Mech.* **764**, 171 (2015).
- [16] See Supplemental Material at <http://link.aps.org/supplemental/10.1103/PhysRevLett.126.118002> for more details on the simulation method and model derivation, and additional numerical data.
- [17] O. Pouliquen and Y. Forterre, A non-local rheology for dense granular flows, *Phil. Trans. R. Soc. A* **367**, 5091 (2009).
- [18] E. Azéma and F. Radjaï, Internal Structure of Inertial Granular Flows, *Phys. Rev. Lett.* **112**, 078001 (2014).
- [19] Q. Zhang and K. Kamrin, Microscopic Description of the Granular Fluidity Field in Nonlocal Flow Modeling, *Phys. Rev. Lett.* **118**, 058001 (2017).
- [20] S. Kim and K. Kamrin, Power-Law Scaling in Granular Rheology Across Flow Geometries, *Phys. Rev. Lett.* **125**, 088002 (2020).
- [21] J. Gaume, G. Chambon, and M. Naaim, Microscopic Origin of Nonlocal Rheology in Dense Granular Materials, *Phys. Rev. Lett.* **125**, 188001 (2020).